Proceedings of the
44th IEEE Conference on Decision and Control, and
the European Control Conference 2005
Seville, Spain, December 12-15, 2005

Extremum seeking applied to the plasma control system of the Frascati Tokamak Upgrade

C. Centioli, F. Iannone, G. Mazza, M. Panella, L. Pangione, S. Podda, A. Tuccillo, V. Vitale, L. Zaccarian

Abstract— **In this paper we will report on the experimental results arising from the implementation of extremum seeking techniques to maximize in real time the RF power coupled to the plasma in the Frascati Tokamak Upgrade (FTU) experimental facility. The RF under consideration is the Lower Hybrid (LH) and the coupling issue consists in the match between an antenna structure (an array of waveguide, the grill) and a load i.e. the plasma. It can be shown that the reflection coefficient (ratio of the reflected and direct power) is a convex function of the density in front of the grill and then of the plasma-grill distance. The optimization of the coupling level reduces the reflected power thus maximizing the RF effects on the plasma and at the same time avoiding temporary power shutdown to protect the system from the excess of reflection. It is shown in the paper that the proposed extremum seeking technique achieves a satisfactory level of robustness with respect to measurement errors and well performs both in simulation and in experimental tests, thus leading to an improved effectiveness of the RF heating system.**

Keywords: Real Time control, RF Power, Lower Hybrid Waves, Extremum seeking, Plasma Control System, FTU experiments

I. Introduction

Most of today tokamak experiments make use of non-inductive current drive to achieve several tasks, in particular proper shaping of the current profile for the advanced or steady state scenarios and stabilization of MHD activity [5], [6], [8], [4]. The lower hybrid (LH) waves capability of driving current has been widely demonstrated. It is has been shown that LH current drive is an essential tool for steady state operations. One of the main problems to tackle in today and future experiments is to provide an optimum coupling between the antenna (an array of waveguide, also called grill) and the plasma all along the LH pulse. The condition of coupling depends mainly on the electron density and its decay length in the border layers between the main plasma and the first wall (Scrape off Layers, SOL). These, in turn, depend, in a complicated way, on several plasma and first wall parameters. In case of poor coupling, part of the injected power is reflected by the SOL, as represented in Figure 1.

It is acknowledged that the reflected power is a convex function of the edge density and then of the position by moving the antenna in the SOL. The behavior of the reflection coefficients vs the SOL density in a simplified model [2] of the antenna and plasma is shown in Figure 2 by the three lines relative to different density gradients in the case of 90 degree phasing of the grill. The reflected power, besides being not available to the plasma, comes back (mainly to the antenna) and can, above certain limits, cause severe damages to internal components.

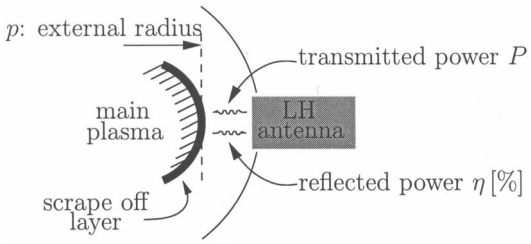

Fig. 1. Transmitted power and its reflection by the SCL.

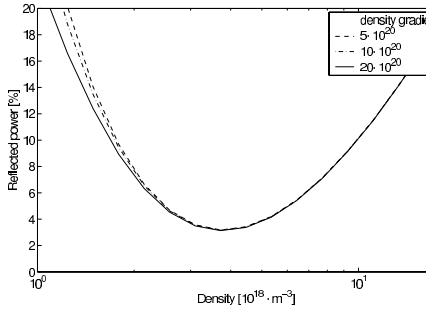

Fig. 2. Reflection coeffi cients vs the SOL density for three different density gradients in the case of 90 degrees phasing of the grill.

At present, in most experiments, the matching condition for the launched waves is obtained using an iterative procedure of moving the antenna in the SOL searching for the minimum reflected power. The unique experiment aiming to a real-time control of the reflected power has been attempted at JET [11]. It was based on the real-time control of the antenna position. It was then abandoned because the real-time control of the antenna position without a suitable control of the interaction with the plasma could cause impurity influx from the antenna itself.

In this work we present a control scheme based on real time control of the plasma position, where the converse idea is applied. Namely, the coupling between the plasma and the antenna is maximized by suitably adjusting the plasma position reference signal processed by the plasma position control system. In particular, based on a measurement of

This work was supported in part by ASI, MIUR (PRIN and FIRB projects) and ENEA-Euratom.

L. Zaccarian and L. Pangione are with the Dipartimento di Informatica, Sistemi e Produzione, University of Rome, Tor Vergata, 00133 Rome, Italy zack@disp.uniroma2.it

C. Centioli, F. Iannone, G. Mazza, M. Panella, S. Podda, A. Tuccillo and V. Vitale are with Associazione Euratom/ENEA sulla Fusione, Centro Ricerche Frascati, CP 65, 00044 Frascati (Roma), Italy.

0-7803-9568-9/05/$20.00 ©2005 IEEE

the reflection coefficient, an extremum seeking algorithm is employed to adjust the plasma position so to reach the optimal coupling. Extremum seeking techniques have been first introduced in the 1950s and correspond to nonlinear dynamic schemes aimed to reaching an extremum of an unknown static map. It was only in recent years that formal stability properties of these control schemes were studied, by way of recent nonlinear tools on averaging and two-time scales systems (see, e.g., [7], [9] and references therein). We report in this paper on the successful application of these techniques to the relevant control problem outlined above, on the experimental facility available at FTU. The paper is structured as follows: in Section II we will describe the problem setting and the adopted extremum seeking scheme. In Section III we will give the simulation results. Finally In Section IV we will report on the experimental tests carried out at FTU.

II. The extremum seeking scheme

The Position and Plasma Current Feedback System (PPCS) running at FTU is currently working under an RTAI-Linux architecture [10]. This control system controls a set of four windings to regulate the plasma current, the plasma internal and external radii and the plasma lower and upper limits. Among other things, based on suitable direct and indirect measurements from the experimental device, the control system adjusts the plasma position based on the deviation from a set of preprogrammed reference signals, following a PID control strategy [3]. In particular, the horizontal position of the plasma is regulated by the controller by adjusting the position of the external radius p based on a reference signal r_p, typically corresponding to a preprogrammed profile. The overall dynamics can be represented as

$$\begin{array}{rcl} \dot{x}(t) & = & f(x(t), r_p(t) + n_i(t)) \\ p(t) & = & h(x(t)), \end{array} \tag{1}$$

where $f(\cdot,\cdot)$ and $h(\cdot)$ are suitable smooth maps and $n_i(t)$ represents noise acting at the plant input. Moreover, when the Lower Hybrid antenna is active, the percentage of reflected power $\eta(t)$ can be modeled as a static function of the plasma position resembling the "U"-shaped curve of Figure 2:

$$\eta(t) = h_U(p(t)) + n_o(t), \tag{2}$$

where $n_o(t)$ represents noise acting at the plant output and $h_U(\cdot)$ is a convex function.

Due to the above commented architecture, it is possible to adjust online the reference position $r_p(t)$ as follows:

$$r_p(t) = \theta(t) + \bar{r}(t), \tag{3}$$

where $\bar{r}(t)$ is the (typically constant) preprogrammed reference for the plasma horizontal position and $\theta(t)$ is a correction term arising from an extremum seeking algorithm aimed at maximizing the plasma vs antenna coupling with the goal of reaching a minimum level of reflected power. Indeed, by adjusting the position of the external radius of the plasma, the edge density accordingly changes and it is therefore possible to reduce the reflected power by seeking for the minimum of the curve in Figure 2. In particular, given a certain edge density of the plasma, a similar curve to that of Figure 2 relates the plasma external radius to the percentage of reflected power (see the simulation and experimental results reported next), so that adjusting the plasma position will lead to the optimization of the plasma vs antenna coupling.

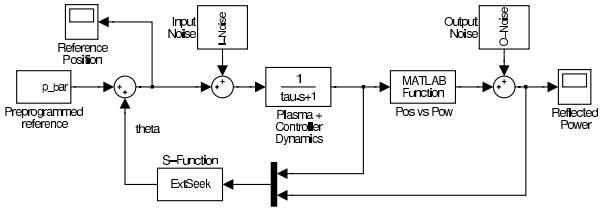

Fig. 3. Simulation diagram for the optimization algorithm.

From the point of view of the required optimization task, the control scheme can be represented by the block diagram of Figure 3. In this diagram, the plasma and controller dynamics are lumped into a single dynamic block whose response time can be estimated around 4 milliseconds. Based on the reference adjustment $\theta(t)$ commanded by the extremum seeking algorithm (therein denoted "Reference Position"), it is possible to simulate the rough variation of the external radius by replacing the complex (but fast!) dynamics in (1) using a first order system with time constant $\tau = 0.004$ seconds:

$$\dot{p}(t) = \frac{1}{\tau}\left(r_p(t) + n_i(t) - p(t)\right). \tag{4}$$

Furthermore, the external radius is fed into a static "U"-shaped function which corresponds to the percentage of reflected power that we wish to minimize, resembling the relation (2). The extremum seeking algorithm is assumed to have access to measurements of both the plasma external radius $p(t)$ and the percentage of reflected power $\eta(t)$, at sampling instants. However, the control scheme is subject to high levels of noise, both acting before the plasma position measurement (input noise n_i) and acting before the reflected power measurement (output noise n_o). Based on experimental data, the input noise has been quantified as the sum of three components consisting of a 50Hz sine wave disturbance, a constant offset and a filtered Gaussian noise with 200 Hz maximum frequency (these disturbances probably arise from the high power circuits of the coil actuators); the output noise has been selected as a filtered Gaussian noise with 2 Khz maximum frequency.

The algorithm implemented in the "ExtSeek" block of Figure 3 is based on the acquisition and processing at each sampling time of the input $p(t)$ and output $\eta(t)$ of the static nonlinearity relating the reflected power to the horizontal plasma position. The algorithm assigns at each sampling time the value of the correction $\theta(t)$ to be added to the preprogrammed reference $\bar{r}(t)$ as in (3). The internal architecture of this block is based on the classical extremum seeking scheme (see, e.g., [7], [9]) represented in Figure 4, wherein a sinusoidal signal is added to the input of the static nonlinearity and employed via a demodulator at the

nonlinearity output to detect the sign of the correction signal. This signal is then integrated to guarantee semiglobal practical stability of the scheme (see [7], [9] for details about the stability proofs).

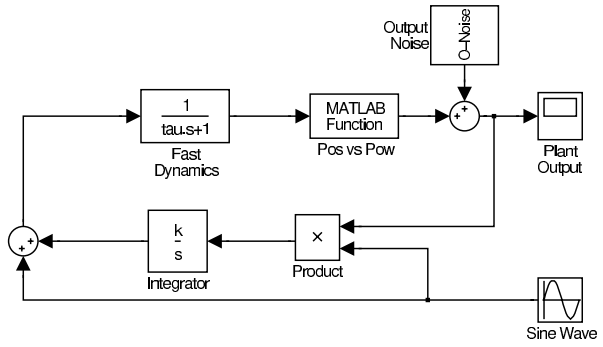

Fig. 4. Extremum seeking scheme.

In our case, due to safety reasons on the experimental device, we avoid to introduce the sinusoidal excitation signal represented in Figure 4 and attempt to rely on the existing sinusoidal disturbance $n_i(t)$ introduced at the plant input by the power circuits of the coil actuators. Both simulation and experimental results will illustrate that this disturbance alone is already sufficient to guarantee a successful and reliable extremum seeking task for the minimization of the reflected power. [1]

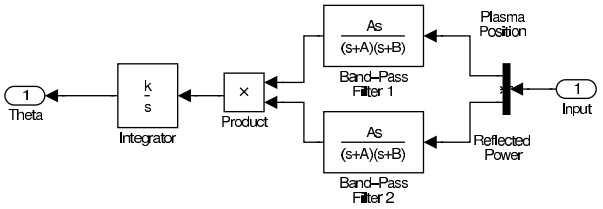

Fig. 5. The algorithm implemented in the "ExtSeek" block of Figure 3.

In particular, the internal architecture of the "ExtSeek" block of Figure 3 is shown in Figure 5, which corresponds to an approximation of the classical extremum seeking scheme where the sinusoidal signal is reconstructed by filtering the plasma position $p(t)$ through a band pass filter with lower and upper cutoff frequencies $\omega_l = 2\pi f_l$ and $\omega_h = 2\pi f_h$, respectively, as follows:

$$\frac{p_f(s)}{p(s)} = \frac{\omega_h s}{(s+\omega_h)(s+\omega_l)}. \tag{5}$$

An exact copy of the same filter is applied to the measured reflected power $\eta(t)$, both to filter out the output disturbance $n_o(t)$ (following the same technique as in [7]) and to preserve the synchronization of the two signals before the product.

$$\frac{\eta_f(s)}{\eta(s)} = \frac{\omega_h s}{(s+\omega_h)(s+\omega_l)}. \tag{6}$$

Finally, based on the filtered values $\eta_f(t)$ and $p_f(t)$, the extremum seeking algorithm corresponds to selecting the correction term $\theta(t)$ as follows:

$$\dot{\theta}(t) = k\,\eta_f(t)p_f(t). \tag{7}$$

Note that the scheme of Figures 3 and 5, corresponding to equations (1), (2), (3), (5), (6), (7) has slight differences from the classical scheme of Figure 4. Nevertheless, the stability results of [7] and [9] still apply as the averaging techniques are independent on the position of the fast dynamics and the subsequent singular perturbation reasoning can be applied in a straightforward manner also to our case. As pointed out in [7] and later confirmed in [9], the system has three time scales corresponding to 1) fastest: the plant with the stabilizing controller (1); 2) medium: the period of the sinusoidal perturbation; 3) slow: the variation speed of the adaptation $\theta(t)$ (which increases with k). In our case, since the frequency of the sinusoidal signal present at the plant input is fixed (and significantly slower than the plant dynamics), the result in [7], which holds under mild conditions on the plant (1), guarantees that there exists a small enough value k^* such that for all $k \in (0, k^*)$ the closed-loop (1), (2), (3), (5), (6), (7) has a unique exponentially stable periodic solution whose size is upper bounded by the size of the sinusoidal disturbance and by the level of time scale separation among the different systems. [2] Moreover, based on the recent results in [9], these local stability properties extend to semiglobal ones. It is important to emphasize that the result apply to any (fast enough) nonlinear plant dynamics of the form (1) and that the approximate model (4) is only used for simulation purposes.

III. Simulation results

Prior to experimentation, suitable simulation results have been studied to test the reliability of the extremum seeking scheme. In particular, the control scheme of Figure 3 has been simulated by implementing in the block "ExtSeek" a MATLAB S-function containing the C source code of the control routine prepared for the Linux-RTAI plasma control system.

In our simulations, based on experimental data, we used the following selections for the input and output noise:

$$\begin{aligned} n_i(t) &= 0.001\,\sin(50\cdot 2\pi t) + n_{gi}(t) - 0.002 \\ n_o(t) &= n_{go}(t), \end{aligned}$$

where $n_{gi}(t)$ and $n_{go}(t)$ are filtered Gaussian noises with variances $3\cdot 10^{-6}$ and $3\cdot 10^{-1}$, respectively, and cutoff frequencies $200\,Hz$ and $2\,KHz$, respectively. Moreover, as previously commented, the plasma position control system (1) has been approximated by a first order dynamic system with time constant $\tau = 0.004$. As for the extremum seeking scheme, to correctly isolate the 50 Hz sinusoidal disturbance at the plant input, the two band pass filters (5), (6) have been selected with cutoff frequencies $\omega_l = 2\pi 20$ and $\omega_h = 2\pi 100$ while different values of the gain k have been tested to achieve a suitable approximation of the critical value k^* and of the best gain to be implemented in the experimental runs.

[1] It would be of course also possible to add an external sinusoidal signal to reproduce the typical extremum seeking scheme of Figure 4.

[2] Due to space constraints, we choose not to describe all the technical details here and rather refer the reader to the papers [7], [9].

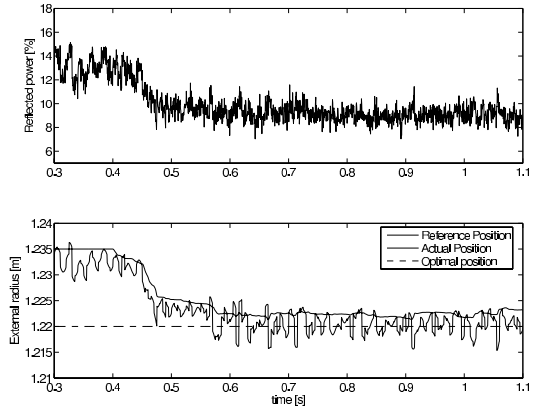

Fig. 6. Algorithm simulation with the selection $k = 140$.

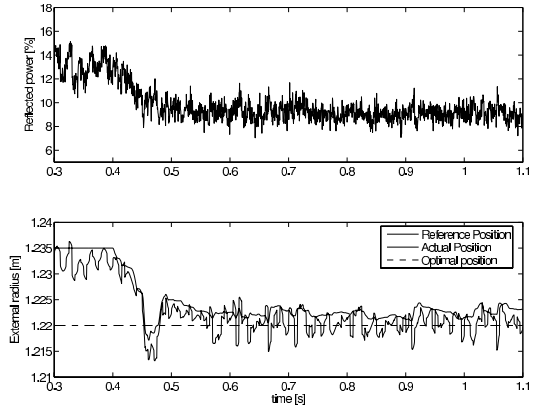

Fig. 7. Algorithm simulation with the selection $k = 500$.

In all the simulations reported in Figures 6, 7 and 8, the extremum seeking algorithm is started at time 0.4 and aims at leading the reflected power percentage (represented in the upper plot) to its minimum of 8%. The lower plots report on the reference position (gray) and the actual position of the plasma (black). Figures 6 and 7 report the simulation results for the two selections $k = 200$ and $k = 500$. Both simulations correspond to a desirable convergence to the optimal position. Note that the average of the actual position presents a small deviation from the reference position, due to the constant component of the input disturbance $n_i(t)$. Since the extremum seeking algorithm is based on the assumption that the plasma position slides along an equilibrium set (i.e., the effect of the time constant τ is disregarded) it is reasonable to expect that there exists a large enough gain k that leads to closed-loop instability. This is actually the case for the simulation of Figure 8 where a gain $k = 3000$ has been used. In this simulation, the closed-loop bounces back and forth between the safety limits imposed to the plasma position reference value, thereby leading to the highly undesirable and oscillatory behavior of Figure 8. In practical implementation, it is quite natural to expect that, due to the unmodeled nonlinearities and uncertainties of the closed-loop, even a scenario such as that of Figure 7 may lead to instability. Indeed, already in this simulation (corresponding to $k = 500$) it is possible to see a very aggressive behavior of the controller, leading to a dangerous undershoot. The recommended gain selection should be somewhere around the value $k = 200$ used in the simulation of Figure 6 as it leads to a graceful convergence to the desired optimal position.

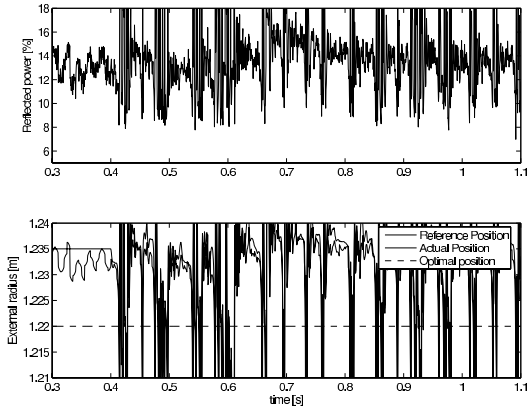

Fig. 8. Algorithm simulation with the selection $k = 3000$.

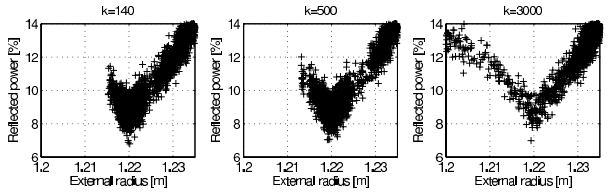

Fig. 9. The "U"-shaped curve for the three simulation studies.

For the three simulations commented above and reported in Figures 6, 7 and 8 we show in Figure 9 the Cartesian representation of the position/power pairs generated by our simulation model. Note that in the case $k = 200$ (left plot), corresponding to the simulation of Figure 6, the algorithm explores almost only one side of the "U"-shaped curve of Figure 2, leading directly to the optimum value. In the case $k = 500$ (middle plot), corresponding to the simulation of Figure 7, the algorithm slides along the right side of the "U"-shaped curve and, due to the aggressiveness of the control action, severely overshoots on the opposite side of the curve. Finally, for the undesirable oscillatory case (right plot), corresponding to the simulation of Figure 8, the algorithm will keep oscillating along both sides of the "U"-shaped curve, in an unacceptable way.

IV. Experimental results

The extremum seeking algorithm described in the previous section has been recently validated on the FTU experimental facility through experiments using one of the six lower hybrid current drives available at FTU [1].

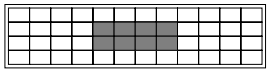

Fig. 10. The 48 cells of the LH emitter terminal matrix.

With the goal of providing the PPCS with a measurement of the reflected power percentage, the open source architecture provided by RTAI-Linux allowed to set-up an

auxiliary real-time module, located close to the LH launcher, which monitors and averages the central eight cells of the emitter terminal matrix (this matrix consists of 4 parallel lines, each of them hosting 12 cells as shown in Figure 10 where the measured ones are shaded in gray). Based on 16 inputs corresponding to the measurements of the emitted and reflected power for each of the 8 cells, the auxiliary real-time module computes one signal corresponding to the percentage of reflected power and sends it to an auxiliary input of the PPCS. This architecture increases the scalability of the system, so that a larger set of measurements could be used by only modifying the auxiliary real-time module. Moreover, no modifications to the backup control systems are needed because only one extra analog input is required by the central plasma position control unit.

In all the experiments, the LH pulse is active in the time interval $t \in [0.3, 1.1]$ seconds. The extremum seeking algorithm is activated at time $t = 0.35$, so that in the interval $[0.3, 0.35]$ it is possible to appreciate the initial level of reflected power to be improved by the algorithm.

We first comment on the experimental result of shot # 26718, where the gain had been fixed as $k = 300$. The corresponding response is reported in Figure 11, where it is possible to check that the algorithm succeeded in significantly reducing the reflected power. However, from Figure 11 it appears that, as compared to the simulation studies, the selection $k = 300$ already leads to a very aggressive control action, which may lead to instability. Moreover, due to a highly disaligned initial position of the antenna, the correction term $\theta(t)$ reaches the safety saturations imposed to the extremum seeking scheme and does not allow to fully appreciate the response behavior.

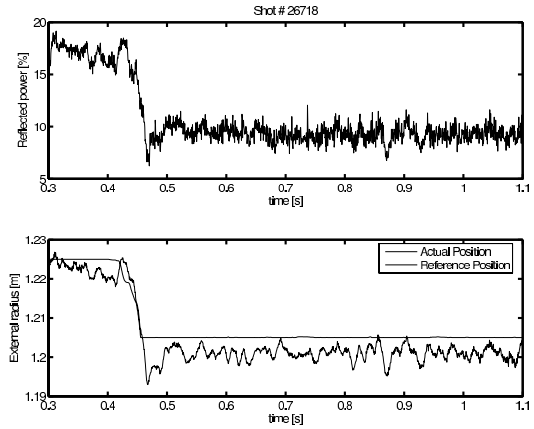

Fig. 11. Shot # 26718 corresponding to the gain $k = 300$, where the algorithm reaches the maximum displacement correction.

In a subsequent experiment, due to the above two reasons, we augment the safety limits imposed to the plasma position allowing to reduce the plasma external radius of one extra centimeter and reduce the gain to $k = 250$. The arising response is represented in Figure 12, where it is possible to appreciate a highly desirable behavior of the algorithm. Indeed, the plasma is gracefully moved to the optimal position thus leading to a gradual reduction of the reflected power from 14% to 6%.

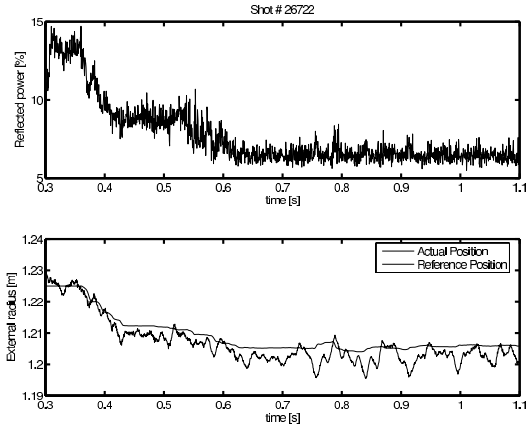

Fig. 12. Shot # 26722 corresponding to the gain $k = 250$.

Before the following experiment, we change the initial position of the antenna so that the minimum of the convex curve is more central within the operational range of the extremum seeking algorithm. In particular, since in Figures 11 and Figures 12 the algorithm aims at reducing the external radius, thereby augmenting the distance between plasma and antenna, we decide to move out the antenna in the radial direction, so that at the optimal position the plasma won't be too compressed at the center of the chamber. With this initial position of the antenna, we first check on the behavior of the algorithm with a higher gain of $k = 350$ and then on its behavior with an smaller gain of $k = 200$, which should be more desirable, given the very aggressive behavior witnessed in the experiment of Figure 11.

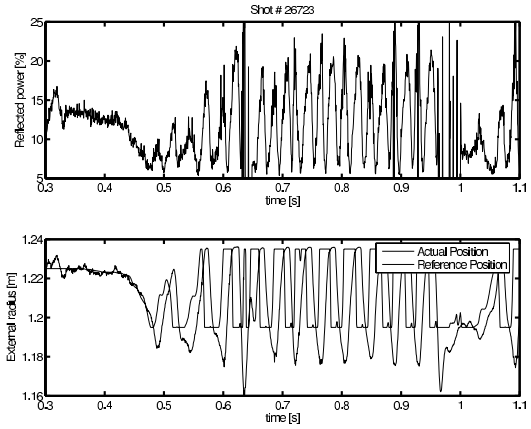

Fig. 13. Shot # 26723 corresponding to the gain $k = 350$, where the algorithm exhibits instability.

The resulting responses are represented in Figures 13 and 14. In the first case the algorithms leads to unacceptable oscillations, thus confirming the intuition that the limit gain k^* commented in Section III is significantly smaller than the one predicted by the simulations studies (this is probably due to unmodeled nonlinearities and uncertainties of the system). In the second case, the gain reduction leads the algorithm back to correct operation and it is possible to appreciate once again a significant reduction of the reflected power.

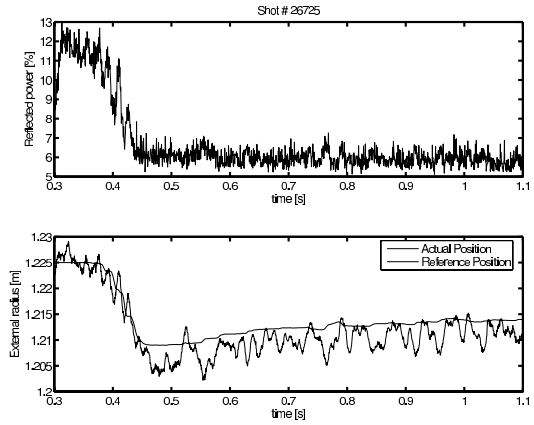

Fig. 14. Shot # 26725 corresponding to the gain $k = 200$.

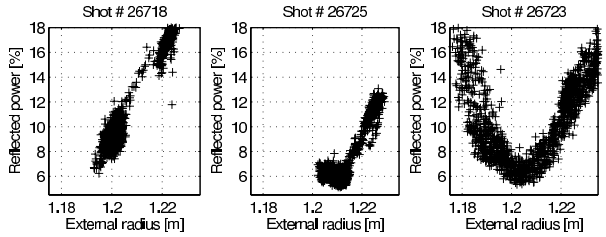

Fig. 15. The "U"-shaped curve for shots # 26718, # 26725 and # 26723.

Parallel to Figure 9 for the simulation studies, we report in Figure 15 the samples of the input output pairs processed by the algorithm in the cases of Figures 11, 13 and 14. From the three plots it appears how in the first case of shot # 26718 (left plot), the safety saturation prevented the algorithm to reach the minimum of the "U"-shaped curve. Instead, in the case of shot # 26725 (middle plot), after the antenna was moved, the algorithm is able to regulate the plasma around the optimal position, by slightly overshooting in the opposite direction. Note also that the shape of the curve has slightly changed after the antenna was moved and, of course, the position of the minimum shifted toward the external direction. Finally, for the unstable shot # 26723 (right plot), the algorithms explores all the "U"-shaped curve by undesirably bouncing between the positive and negative safety saturation values.

Finally, we recall that, as shown in Figure 10, only the eight central cells of the emitter are considered for the optimization algorithm. Nevertheless, the emitted and reflected power by each one of the 48 cells is measured and recorded in the experimental database (even though these signals are not available to the real-time control system). It becomes then important to verify the algorithm's effectiveness on the whole matrix of cells, both for efficiency reasons (thereby the average reflected power becoming relevant), where the concern is to maximize the power absorbed by the plasma and for safety reasons (thereby the maximum reflected power becoming relevant), where the concern is to avoid damage to the equipment or annoying safety shutdowns. In Figure 16, both the maximum and average reflected power for the 48 emitting cells is reported. It becomes evident that the proposed strategy achieves a major increase, both in efficiency and safety of the system. Comparable results apply to the

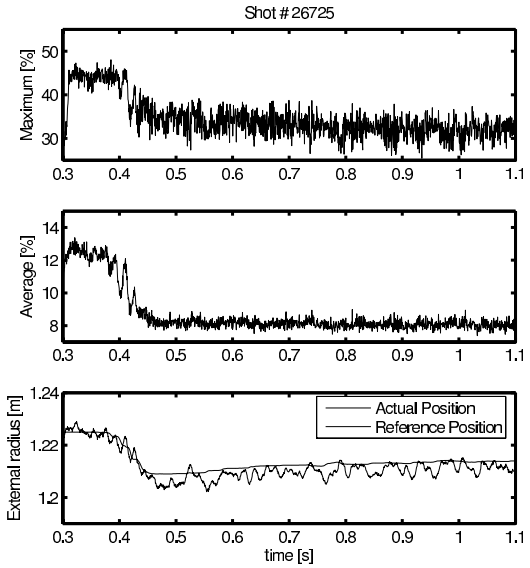

Fig. 16. Maximum and average reflected power on the whole matrix of 48 cells for shot # 26725.

experiments reported in Figures 11 and 12 and are not reported here due to space constraints.

Acknowledgment. The authors wish to thank the FTU operators team for their invaluable assistance during the experimental sessions, Giuseppe Mazzitelli for his encouragement during this work and Dragan Nešić for useful discussions.

REFERENCES

[1] R. Andreani, C. Gourlan, F. Mirizzi, M. Sassi, C. Ferro, A. Marra, A. Orsini, T. Fortunato, and M. Roccon. The 8MW, 8GHZ FTU LHRF system: R&D and design status. In *Proceedings of the 13th Symposium on Fusion Engineering*, Knoxville (TN), USA, October 1989.

[2] M. Brambilla. Slow-wave launching at the lower hybrid frequency using a phased waveguide array. *Nucl. Fusion*, 16:47–54, 1976.

[3] F. Crisanti, C. Neri, and M. Santinelli. FTU plasma position and current feedback. In *Proceedings of the 16th Symposium on Fusion Technology*, London (UK), September 1990.

[4] C.D. Warrick *et al.* Complete stabilization of neoclassical tearing modes with lower hybrid current drive on COMPASS-D. RF teams. *Phys Rev Lett.*, 85(3):574–7, July 2000.

[5] F. Crisanti *et al.* JET quasistationary internal-transport-barrier operation with active control of the pressure profile. *Phys Rev Lett.*, 88(14):145004, April 2002.

[6] T. Fujita *et al.* Quasisteady high-confinement reversed shear plasma with large bootstrap current fraction under full noninductive current drive condition in JT-60U. *Phys Rev Lett.*, 87(8):085001, August 2001.

[7] M. Krstic and H.H. Wang. Stability of extremum seeking feedback for general nonlinear dynamic systems. *Automatica*, 36(4):595–601, 2000.

[8] X. Litaudon and Tope Supra Equipe. Stationary regimes of improved confinement in Tore Supra. *Plasma Phys. Control Fusion*, 38(9):1603–1626, September 1996.

[9] Y. Tan, D. Nešić, and I.M.Y Mareels. On non-local stability properties of extremum seeking control. *Automatica*, 2005, to appear.

[10] V. Vitale, C. Centioli, F. Iannone, G. Mazza, M. Panella, L. Pangione, S. Podda, and L. Zaccarian. Real-time linux operating system for plasma control on FTU: Implementation advantages and first experimental results. *Fusion Engineering and Design*, 71:71–76, June 2004.

[11] C.I. Walker, C. Gormenzano, A. Kaye, M.Lenholm, P.Paling, R. Price, and P. Shild. Real-time position control of the JET LHCD launcher. In *Proceedings of the 17th Symposium on Fusion Technology*, pages 671–675, Rome, Italy, September 1992.